HHS Public Access

Author manuscript

Adv Funct Mater. Author manuscript; available in PMC 2017 October 26.

Published in final edited form as:

Adv Funct Mater. 2016 October 18; 26(39): 7057–7066. doi:10.1002/adfm.201602808.

Multifunctional Photonics Nanoparticles for Crossing the Blood–Brain Barrier and Effecting Optically Trackable Brain Theranostics

Dr. Ajay Singh,
Center for Theragnosis and Center for Neuro-Medicine, Korea Institute of Science and Technology (KIST), Seoul 136-791, South Korea. Institute for Lasers Photonics and Biophotonics, Department of Chemistry State University of New York, Buffalo, NY 14260, USA

Dr. Woong Kim,
Center for Theragnosis and Center for Neuro-Medicine, Korea Institute of Science and Technology (KIST), Seoul 136-791, South Korea

Youngsun Kim,
Center for Theragnosis and Center for Neuro-Medicine, Korea Institute of Science and Technology (KIST), Seoul 136-791, South Korea

Dr. Keunsoo Jeong,
Center for Theragnosis and Center for Neuro-Medicine, Korea Institute of Science and Technology (KIST), Seoul 136-791, South Korea

Dr. Chi Soo Kang,
Center for Theragnosis and Center for Neuro-Medicine, Korea Institute of Science and Technology (KIST), Seoul 136-791, South Korea

Dr. YoungSoo Kim,
Center for Theragnosis and Center for Neuro-Medicine, Korea Institute of Science and Technology (KIST), Seoul 136-791, South Korea

Prof. Joonseok Koh,
Department of Organic and Nano System Engineering Konkuk University Seoul 143-701, South Korea

Prof. Supriya D. Mahajan,
Department of Medicine Division of Allergy, Immunology, and Rheumatology State University of New York Clinical Translational Research Center Buffalo, NY 14203, USA

Prof. Paras N. Prasad, and
Institute for Lasers Photonics and Biophotonics Department of Chemistry State University of New York Buffalo, NY 14260, USA

Dr. Sehoon Kim

Correspondence to: Paras N. Prasad; Sehoon Kim.

Supporting Information

Supporting Information is available from the Wiley Online Library or from the author.

Center for Theragnosis and Center for Neuro-Medicine, Korea Institute of Science and Technology (KIST), Seoul 136-791, South Korea

Abstract

Theranostic photonic nanoparticles (TPNs) that cross the blood–brain barrier (BBB) and efficiently deliver a therapeutic agent to treat brain diseases, simultaneously providing optical tracking of drug delivery and release, are introduced. These TPNs are constructed by physical encapsulation of visible and/or near-infrared photonic molecules, in an ultrasmall micellar structure (<15 nm). Phytochemical curcumin is employed as a therapeutic as well as visible-emitting photonic component. In vitro BBB model studies and animal imaging, as well as ex vivo examination, reveal that these TPNs are capable of transmigration across the BBB and subsequent accumulation near the orthotopic xenograft of glioblastoma multiforme (GBM) that is the most common and aggressive brain tumor whose vasculature retains permeability-resistant properties. The intracranial delivery and release of curcumin can be visualized by imaging fluorescence produced by energy transfer from curcumin as the donor to the near-infrared emitting dye, coloaded in TPN, where curcumin induced apoptosis of glioma cells. At an extremely low dose of TPN, a significant therapeutic outcome against GBM is demonstrated noninvasively by bioluminescence monitoring of time-lapse proliferation of luciferase-expressing U-87 MG human GBM in the brain. This approach of TPN can be generally applied to a broad range of brain diseases.

1. Introduction

The blood–brain barrier (BBB) is a cellular barrier composed of tight junctions between vascular endothelial cells interfaced with associated pericytes and astrocytes, the barrier function of which protects the central nervous system (CNS) by regulating the entry of nutrients and other substances to the brain. [1,2] Because of this vascular barrier, most CNS drugs have shown low efficiencies for transcranial delivery; thus, to compensate, they are generally administered at very high doses, which results in severe side effects in peripheral organs. [3] For this reason, efficient BBB-crossing brain delivery systems are in high demand to ensure the therapeutic outcome of chemodrugs, while avoiding their adverse systemic effects. In this study, we introduce biocompatible multifunctional theranostic photonic nanoparticles (TPNs) that are capable of crossing the BBB, delivering a therapeutic agent to the CNS, and being self-traceable upon systemic administration. TPNs are ultrasmall molecular nanoparticles constructed by physical assembly of Pluronic (F-127) and photonic molecules. Pluronic, a triblock polymeric amphiphile, was chosen as a colloidal surface constituent because a family of Pluronic surfactants is known to facilitate BBB crossing of drugs and nanoparticles by various proposed mechanisms. [4–6] In vitro and animal models of the intact BBB were used to show efficient transcranial migration of TPNs across the BBB.

Theranostics that combines both diagnostic and therapeutic capabilities in a single material platform has shown great potential in diagnosis, therapy, and real-time monitoring of therapeutic responses. [7,8] To demonstrate the theranostic potential of TPN, we have chosen glioblastoma multiforme (GBM) as a CNS disease model. GBM is the most frequent and

aggressive brain tumor, with poor prognosis and a considerably low survival rate. [9] Owing to its high resistance to numerous anticancer agents, malignant GBM patients have not yet profited from chemotherapy. It is known that the BBB in GBM is partially disrupted. [10] However, the disrupted vasculature of GBM does not assure clinically relevant penetrance of therapeutics. Tumor-associated BBB disruption is highly heterogeneous, depending on the location in GBM (tumor core or periphery). [11] Moreover, the vessel state of GBM is dynamic and maintains permeability-resistant BBB properties to a significant extent, remaining as a major obstacle to the systemic chemotherapy of GBM. [12] Hence, there are continuing needs to develop nanoformulations that can cross the BBB to increase the intracranial concentration of drugs with anti-GBM activity. The capability of TPN to extravasate through the intact BBB, as outlined in this study, will help achieve optimal pharmacokinetics of anti-GBM agents by efficient brain delivery.

Another major impediment to GBM therapy is a lack of methods for monitoring the successful transcranial drug delivery and therapeutic responses of the tumor, except for autopsy. Recently, we reported an optical monitoring method using an orthotopic GBM mouse model with intracranial xenografts of luciferase-expressing GBM cells, with which therapeutic effects of the intraperitoneally-injected curcumin could be monitored noninvasively by bioluminescence imaging (BLI) of the tumor in the brain. [13] In this earlier study, curcumin was used as a safe natural product that can inhibit tumor growth via multiple mechanisms. [13–15] Besides its biological activities, curcumin has characteristic photonic functions. As a yellow hydrophobic polyphenol agent found in turmeric (Figure 1a), curcumin has light absorption and emission in the visible range, which may render it self-traceable with its own photonic signal to allow for monitoring its delivery in vivo. However, in spite of these versatilities, clinical applications of curcumin have been limited because of its short biological half-life, poor solubility, and low bioavailability. [16]

In the study reported here, curcumin was employed as an optically self-signaling anticancer ingredient, and incorporated into TPN to be delivered to the brain and provide theranostics for GBM. The coencapsulated photonic molecule (CbV, Figure 1a), which was developed in our previous work, has strong solid-state fluorescence (SSF) in the highly tissue-penetrating near-infrared (NIR) region and enhanced the optical signal from TPN for in vivo uses. [17] The structure of TPN was engineered to form a stable aqueous dispersion of ultrasmall colloids (<15 nm in diameter) that are composed of hydrophobic photonic molecules in the interior and stabilized with the amphiphilic F-127 on the surface (Figure 1b). Here, we report the in vitro and in vivo evaluations on the BBB-crossing and transcranial GBM-targeting behavior of TPN. The self-traceable photonic activity of curcumin and its energy-transferring interaction with the coassembled CbV dye in TPN were found to enable sequential in vivo visualization of the transcranial delivery of TPN-loaded curcumin and its release to the brain. A significantly enhanced in vivo efficacy of GBM treatment by curcumin-loaded TPN, compared to a solution of free curcumin, was also demonstrated by bioluminescence monitoring, along with in vitro evaluation on the anticancer activity of curcumin against brain cancer cells.

2. Results and Discussion

Multiple-molecule-integrated TPN was formulated by following our reported method. [17,18] Briefly, photonic molecules (curcumin and/or CbV) were homogeneously mixed with F-127 in solution, and water was added to the dried mixture. During the latter step, homogeneously dispersed colloids were spontaneously formed in water. No apparent precipitates were observed in the dispersion, suggesting that water-insoluble photonic molecules were fully embedded in the hydrophobic interior of the self-assembled nanostructure of amphiphilic F-127. Three types of TPN samples were prepared with different compositions of (i) F-127/ curcumin (curcumin-encapsulated nanoparticles, TPN-cur), (ii) F-127/CbV (TPN-CbV), and (iii) F-127/ curcumin/CbV (TPN-cur/CbV), where TPN-CbV has been reported in our previous work as a systemic tumor imaging nanoprobe with high-contrast NIR SSF. [17] As shown in Figure 1c, transmission electron microscopic (TEM) imaging revealed that the obtained TPN colloids are spherical nanoparticles with average diameters of 11 ± 2.5 nm (TPN-cur), 10 ± 1.2 nm (TPN-CbV), and 14 ± 1.7 nm (TPN-cur/CbV). The number-weighted hydrodynamic sizes were measured to be smaller than 20 nm for all TPNs (see Figure S1 in the Supporting Information). These colloidal sizes are small enough to facilitate circulation in the bloodstream and are thus appropriate for systemic applications. [19]

Figure 2a,b shows the visible-to-NIR optical properties of TPNs determined by the photonic molecules entrapped therein. Water-dispersed TPN-cur presented the characteristic visible absorption and fluorescence of curcumin, as typically observed in organic solution. This indicates successful loading of curcumin in the hydrophobic interior of Pluronic nanoparticles. Dye-concentrated TPN-CbV showed efficient NIR light emission without self-quenching of fluorescence, typical of the SSF behavior of CbV. [17] When curcumin and CbV are coloaded in the nanoscopic space (TPN-cur/CbV), the curcumin emission is efficiently quenched while the CbV emission is amplified under photoexcitation of curcumin at 450 nm, suggesting that the absorbed photon energy transfers from curcumin to CbV. Such an efficient energy transfer is attributable to the high intraparticle density of the energy acceptor (CbV) and its close proximity to the coloaded energy donor (curcumin). This nanophotonic interaction between curcumin and CbV was used for noninvasive in vivo monitoring of the therapeutic cargo (curcumin) release by imaging the alteration in the energy-transferred emission of TPN-cur/CbV at ≈700 nm.

To assess the possibility of brain targeting by TPNs, the BBB permeability was quantitatively measured by using a cell-based in vitro transwell model of the BBB that was validated in our previous study. [20] In the two-chamber transwell system, primary cultured human brain microvascular endothelial cells (BMVECs) and normal human astrocytes (NHAs) were grown on the opposite sides of a semipermeable membrane insert that separates luminal and abluminal compartments (Figure 3a). After adding samples in the upper chamber (luminal), the extents of time-dependent transmigration to the lower chamber (abluminal) were determined by measuring the relative light absorption of each sample. As shown in Figure 3b, it turned out that all three TPNs are able to cross the intact BBB with similar profiles of percentage transmigration. Because of the structural similarity in terms of colloidal size and Pluronic surface nature, it is likely that TPNs follow an identical transport route through the BBB. A plausible mechanism is passive endocytosis-mediated

transendothelial migration enhanced by Pluronics, which is promoted through inhibition of the P-glycoprotein drug efflux activity in the BBB (effected by energy depletion and membrane fluidization) and/or increased vesicular transport by the micellar structure. [4–6] To our interest, a non-particulate disseminated form of rhodamine-labeled Pluronic itself without nanoassembly (F-127-Rh solution, Scheme S1, Supporting Information) showed a significantly lower BBB-crossing efficiency than particulate TPNs, suggesting that the formation of the Pluronic nanostructure and its Pluronic-rich colloidal surface play a critical role in facilitating endocytosis by endothelial cells, thus enhancing the transcellular migration across the BBB.

To monitor the temporal cargo release from TPNs, changes in the absorption spectra were examined during the period of time given in Figure 3b (see Figure S2 in the Supporting Information). TPNs (TPN-CbV, TPN-cur, and TPN-CbV/cur) were dispersed in PBS (phosphate buffered saline, pH 7.4) and incubated at 37 °C during the monitoring. In the case of TPN-CbV, the characteristic absorption spectrum of CbV was retained for 36 h, implying stable nanoparticulate encapsulation of CbV with minimal release. In contrast, the absorption band of curcumin in TPN-cur gradually decreased in the course of time, reaching ≈50% of the initial absorbance after 36 h of incubation. A similar behavior was observed for the spectral evolution of TPN-CbV/cur, where the CbV band was maintained while that of curcumin diminished. It was reported that an aqueous solution of curcumin shows considerably weaker absorption at 420 nm than its organic solutions. [21] Considering this, a gradual decrease in the curcumin absorption, observed during the incubation of TPN-cur and TPN-CbV/ cur, strongly suggests that sustained release of curcumin to the aqueous media occurs under the given condition. However, it should be noted that the released free curcumin has very low BBB permeability, as evidenced by the in vivo transcranial migration assessment showing marginal brain accumulation of free curcumin when administered intraperitoneally (see Figure S3 in the Supporting Information). Therefore, the efficient BBB crossing of curcumin and CbV, observed in Figure 3b, is unambiguously attributed to the delivery by Pluronic-based TPNs.

Next, we investigated in a normal mouse model whether TPNs are indeed able to enter the brain across the BBB via systemic administration. As shown in the whole-body fluorescence images (Figure 4a,b), both the intravenously injected TPN-CbV and TPN-cur selectively brightened the brains with optical signals characteristic of CbV and curcumin, respectively. Ex vivo imaging of the resected major organs reveals that most of the TPN populations were localized in the brain, and that filtration by the reticuloendothelial system (RES), such as liver and spleen, is insignificant for both nanoparticles (Figure 4c,d). It is noted that TPN-CbV displayed unexpectedly high lung accumulation, which is not the case for TPN-cur (Figure S4 in the Supporting Information). In spite of their distinct biodistributions, it is evident that both TPNs were efficiently localized in the brain due to their high BBB permeability. Such selective brain accumulation confirms that the intravenously-injected TPNs are capable of long blood circulation with minimal RES clearance and indeed are able to be successfully delivered to the brain across the BBB, as anticipated from our design strategy for TPNs based on ultrasmall colloidal size and Pluronic-rich surface characteristics. In contrast to the nanostructured TPNs, a nonparticulate disseminated form of NIR dye-labeled Pluronic (F-127-Cy5.5 solution, Scheme S2, Supporting Information)

showed no notable sign of brain accumulation upon intravenous injection (see Figure S5 in the Supporting Information). This result is consistent with the low BBB-crossing efficiency of F-127-Rh solution observed in the in vitro model study (Figure 3b), again validating the significance of Pluronic nanostructure formation for accomplishing efficient luminal-to-abluminal transmigration across the BBB.

In the photon-limiting in vivo condition, TPN-CbV that emits bright fluorescence in the NIR manifested better brain signals over the background than visible-light-emitting TPN-cur. As shown in Figure 4a, the in vivo brain signal of TPN-CbV slowly increased to reach a maximum at 2–3 h postinjection and persisted thereafter, indicating that the brain-delivered TPN-CbV stays longer in the brain. In contrast, TPN-cur showed much faster accumulation and clearance of the brain signal (Figure 4b). This implies that curcumin molecules are readily released out of the transcranially delivered TPN-cur and subjected to fast clearance from the brain.

To verify the occurrence of curcumin release from the brain-delivered TPN, we utilized the self-traceable capability and energy-transferring characteristics of the donor/acceptor coloaded TPN (TPN-cur/CbV). The intracranial curcumin release was monitored using a comparative in vivo imaging of its acceptor (CbV) emission by direct excitation and by energy-transferred indirect excitation. As in the case of TPN-CbV and TPN-cur, the coloaded TPN-cur/CbV also displayed selective brain accumulation upon intravenous injection into a normal mouse (Figure 5a,b). Interestingly, brain signaling of the CbV emission presented notably different temporal profiles, depending on the excitation condition. Under the acceptor excitation at 640 nm, the directly excited CbV emission manifested slow accumulation in the brain to reach the maximum intensity at 2–3 h postinjection (Figure 5a), similar to that of TPN-CbV shown in Figure 4a. In the case of donor (curcumin) excitation at 500 nm, however, the brain signal of the energy-transferred CbV emission reached the maximum faster than the former case, at 1 h postinjection, and then faded (Figure 5b). Figure 5c compares such distinct temporal profiles observed from the same TPN-cur/CbV. It reveals that the energy-transferred CbV emission by donor excitation is initially stronger than the directly excited CbV emission, attributable to the acceptor emission amplification by an efficient intraparticle energy transfer from the coloaded donor. However, such an amplified acceptor emission disappeared after reaching the maximum intensity at 1 h postinjection; thereafter, the energy-transferred CbV emission became weaker than the directly excited emission. This reversal of relative intensity indicates that CbV and curcumin are initially colocalized in the same nanospace to yield efficient energy transfer, but undergo separation with time, likely due to the disruption of nanostructure in the brain and concomitant release of curcumin from TPN-cur/CbV. Importantly, emission of the donor (curcumin) itself was shown to keep increasing with time in the brain (see Figure S6 in the Supporting Information). This behavior indicates that the donor emission initially quenched by the intraparticle energy transfer is gradually recovered by separation from the acceptor, further supporting the occurrence of curcumin release in the brain.

We then evaluated whether TPN can target the intracranial glioblastoma tumor across the BBB. An orthotopic mouse model of luciferase-expressing U-87 MG human GBM tumor

that emits bioluminescence upon intraperitoneal injection of luciferin was used to allow for noninvasive detection of tumor size and position in the brain. In this GBM-bearing mouse, it was shown that the signal of intravenously injected TPN-CbV does not visualize the whole brain evenly, but rather focuses on some part of the brain, which seems to localize near the bioluminescent GBM tumor (Figure 6). This in vivo finding is in accordance with the ex vivo brain section imaging that showed close proximity between the localized CbV signal and the intracranial GMB location (see Figure S7 in the Supporting Information). These observations suggest that BBB-crossable TPNs are further capable of preferential accumulation near the tumor with tissue abnormalities.

The preferential GMB targeting and intracranial curcumin release by TPN may offer a new therapeutic opportunity for brain cancers. To demonstrate the anticancer activity of the curcumin-loaded TPNs against GBM, we performed a colony-forming assay (CFA) that serves as a useful tool to test whether a given cancer therapy can reduce the clonogenic survival of tumor cells. [22] First, rat C6 malignant glioma cells were treated overnight with TPN-CbV, TPN-cur/CbV, and free curcumin. Then, the sample-treated or untreated cells were incubated for colony formation, and the number of colonies formed was counted on the 7th day of incubation with crystal violet staining (Figure 7). The counted number of colonies for the cells treated with curcumin-free TPN-CbV (105 ± 5.2) revealed no significant difference from that of the untreated cells (111 ± 5.5), indicating minimal cytotoxicity of the TPN carrier itself. In contrast, treatment with free curcumin caused a significant reduction in the colony counting (78.0 ± 3.9), confirming the therapeutic effect of curcumin. [13–15] The cells treated with curcumin-loaded TPN-cur/CbV presented a considerably further decline in the colony formation (57.5 ± 2.9). From these results, it is unambiguously speculated that the observed anticancer activity of TPN-cur/CbV against glioma cells comes from the loaded curcumin molecules that are efficiently internalized into cells and then released by the TPN carrier.

To gain insight into the resulting anticancer effect, the expression level of proapoptotic protein, Bcl-xS, was evaluated by immunofluorescent staining. Compared to the untreated control, a significant increase in Bcl-xS expression was observed in the glioma cells treated with curcumin as well as with TPN-cur/CbV (see Figure S8 in the Supporting Information), providing evidence that apoptosis cascades were triggered by curcumin. Curcumin-induced apoptosis is known to depend on various factors, among which TNF-α and NF-κB are representative. [13–15] To quantify their gene expression levels, we performed real-time PCR (polymerase chain reaction), where results are expressed as transcript accumulation index (TAI). As shown in Figure 8a, we observed a significant decrease in TNF-α gene expression in glioma cells treated with curcumin (TAI = 0.36 ± 0.047; 64% decrease, $p < 0.01$) and TPN-cur/CbV (TAI = 0.57 ± 0.043; 43% decrease, $p < 0.05$) compared to the untreated control. Conversely, the NF-κB gene expression level was remarkably increased by treatment with curcumin (TAI = 2.52 ± 0.016; 152% increase, $p < 0.01$) and TPN-cur/CbV (TAI = 2.31 ± 0.017; 131% increase, $p < 0.01$) (Figure 8b). Such cellular responses are attributable to the fact that the mechanism underlying the anticancer activity of curcumin includes antiinflammatory responses reflected by a significant decrease in TNF-α gene expression and the activation of NF-κB gene expression that triggers the apoptotic cascade of glioma cells. The cur-cumin-induced anticancer activity could be further verified by the 3-

[4,5-dimethylthiazol-2-yl]-2,5-diphenyltetrazolium bromide (MTT) cell viability assay, revealing that curcumin-loaded TPNs (TPN-cur and TPN-cur/CbV) have dose-dependent cytotoxicity against glioma cells, while the toxicity of blank F-127 itself is negligible (see Figure S9 in the Supporting Information). All these in vitro results suggest that TPNs are a safe and effective nanocarrier to deliver curcumin for brain cancer therapy.

Finally, we performed the in vivo experiment of brain cancer therapy in an orthotopic mouse model of luciferase-expressing U-87 MG human GBM tumor whose bioluminescence allows for noninvasive monitoring of time-lapse proliferation of GBM in the brain. [13,23] Curcumin-loaded TPN-cur was administered daily by intravenous injection for three weeks at a curcumin dose of 0.2 mg kg^{-1} d^{-1} from the third day onward after tumor cell implantation in the brain. In a curcumin-negative control group, a water solution of disseminated blank F-127 was administered in parallel at a dose of the same F-127 amount in TPN-cur applied in the curcumin-positive group. All the treated mice were then subjected to in vivo monitoring of therapeutic responses by luciferin-induced BLI without photoexcitation on days 7, 14, and 21 (Figure 9a). As summarized in Figure 9b, the tumor bioluminescence signal that reflects tumor size and viability was in a similar range for both groups on day 7. In the course of time, however, it increased remarkably in the curcumin-negative control group, unambiguously due to the growth of GBM xenograft in the brain. The facile tumor growth in the control group confirms that disseminated blank F-127 by itself is nontoxic and incapable of crossing the BBB. In sharp contrast, treatment with TPN-cur led to a significant reduction in the tumor bioluminescence with time, evidencing the tumor regression by the brain-delivered curcumin. On day 21, the TPN-treated group showed a nine-fold lower signal of GBM proliferation than the control group, indicating that because of the efficient brain delivery of curcumin by TPN, the anti-GBM therapeutic efficacy is significant even at a low curcumin dose of only 0.2 mg kg^{-1} d^{-1}. This curcumin dosage is ≈1800 times lower than the effective dose of free curcumin in dimethyl sulfoxide (DMSO) solution reported under the same treatment condition; even at such a high dose (360 mg kg^{-1} d^{-1}), free curcumin could not lead to tumor regression but only slowed down the tumor growth (Figure 9b). [13] The extremely low effective dose of curcumin achieved in this study proves the validity of our strategy for brain cancer theranostics based on Pluronic-surfaced ultrasmall TPN colloids capable of systemic brain delivery across the BBB.

3. Conclusion

We have developed self-traceable molecular photonic brain TPNs that are capable of crossing the BBB upon systemic administration, and thereby brain delivery of a therapeutic cargo for GBM treatment. The construction of TPNs is based on the physical integration of F-127 and photonic molecules into self-assembled ultrasmall nanoparticles with a Pluronic-rich colloidal surface. The BBB-crossing and transcranial GBM-targeting capabilities of TPNs were evaluated in vitro as well as in vivo. We identified curcumin to be a self-traceable photonic molecule that is useful for brain cancer theranostics when delivered to the brain by TPN. The self-traceable and energy-transferring photonic functions of donor/acceptor coloaded TPN (TPN-cur/CbV) allowed us to reveal that the transcrani-ally delivered TPN releases curcumin to the brain to induce an effective therapeutic action on GBM. In vitro studies confirmed that curcumin is indeed able to induce apoptosis of brain

cancer cells following a mechanism involving antiinflammatory responses. By virtue of the combined merits of the anticancer activity of curcumin and its efficient delivery to the brain across the BBB, along with photonic self-traceability, curcumin-loaded TPN presented a significantly enhanced therapeutic outcome against GBM at an extremely low effective dose, holding great potential for brain cancer theranostics. This approach can be generalized to apply to a great number of brain diseases and disorders, which we plan to pursue.

4. Experimental Section

Materials

Curcumin, Pluronic F-127 and 5(6)-carboxy-X-rhodamine *N*-succinimidyl ester were purchased from Sigma-Aldrich and used without further purification. MTT and PBS buffer were also obtained from Sigma Aldrich Co. and used as received. Vinylsulfone functionalized Cy5.5 (FPR-675) was obtained from BioActs Co. Ltd. and used as received. Other chemicals and reagents were used as received.

Conjugation of Pluronic F-127 with Dyes

For near-infrared (NIRF)/ visible fluorescence labeling of F-127, vinyl sulfone functionalized Cy5.5 (0.5 mg) or 5(6)-carboxy-X-rhodamine *N*-succinimidyl ester (0.5 mg) were conjugated, respectively, to the hydroxyl group of F-127 (100 mg) by mixing in PBS (pH 8.0) for 24 h at room temperature (Schemes S1 and S2, Supporting Information). The Cy5.5/rhodamine-labeled F-127 was dialyzed against Milli-Q water to remove unreacted low-molecular-weight dyes in a cellulose ester membrane (Spectra/Por membrane, MWCO: 3.5 kDa) for 1 d and then lyophilized.

Preparation and Characterization of TPNs

TPN-cur were prepared by mixing 0.1 mg of curcumin and 20 mg of F-127 in 0.5 mL dichloromethane, after which the solvent was evaporated by air flow. The dried mixture was resuspended in 2 mL deionized water under sonication for a few seconds to afford a clear aqueous dispersion of TPN-cur with a concentration of 50 μg mL^{-1}. TPN-CbV and TPN-cur/ CbV were prepared in a similar way by using 0.2 mg of CbV (NIR dye), with and without the addition of 0.1 mg of curcumin, respectively. The nanoparticle size distribution in deionized water was determined by a dynamic light scattering method using a particle sizer (90Plus, Brookhaven Instruments Corp.) at 25 °C. TEM images of negatively stained particles (with 2 wt % uranyl acetate) were obtained with a CM30 electron microscope (FEI/ Philips) operated at 200 kV. From the TEM images, 60 particles were counted for the size analysis of each sample. Absorption and emission spectra were acquired using a UV–visible spectrometer (Agilent 8453) and a fluorescence spectrophotometer (Hitachi F-7000, wavelength calibrated for excitation and emission), respectively.

Cell Culture

Dulbecco’s Modified Eagle’s medium (DMEM), fetal bovine serum (FBS), and penicillin/ streptomycin were obtained from Gibco (Grand Island, NY, USA). U-87 MG human GBM cell line was obtained from the Korean Cell Line Bank (Seoul, Korea) and maintained in DMEM supplemented with 10% FBS and 1% penicillin/streptomycin in a humidified 5%

CO_2 incubator at 37 °C. Rat C6 malignant glioma cells were obtained from American Type Culture Collection (ATCC) (Cat # ATCC CCL-107) and maintained in F-12 medium, supplemented with 10% FBS and 1% penicillin/streptomycin in a humidified 5% CO_2 incubator at 37 °C.

Preparation of Luciferase Expressing U-87 MG Cells

The U-87 MG cell line was transfected with an adeno-associated viral vector, pGL4 Vector (Promega, Madison, WI, USA), containing firefly luciferase. Cells were screened for in vitro transfection efficiency by treatment with D-luciferin (VivoGlo Luciferin, Promega, Madison, WI, USA) and fluorescence of luciferin was examined under an IVIS Imaging System. To prevent loss or variation of the expression level of luciferase, tumor cells with consistent passage (3 weeks) were used for intracranial implantation.

Preparation of Mouse Models Bearing Luciferase-Expressing U-87 MG Cells

All animal experiments were carried out in accordance with the guidelines established by Korea Institute of Science and Technology (KIST). Male athymic mice (CAnN.Cg-Foxn1nu/Crl) aged 5 weeks were purchased from Orientbio Inc. (Seongnam, Gyeonggi, Korea) and maintained in a temperature- and light-controlled environment with an alternating 12-h light/dark cycle. The mice were anesthetized by intraperitoneal injection of an anesthetic cocktail composed of 15 mg kg^{-1} Zoletil 50 (Virbac, Carros, France) and 6 mg kg^{-1} Rompun (Bayer HealthCare AG, Leverkusen, Germany), and positioned in a stereotactic device (David Kopf Instruments, Tujunga, CA, USA) using ear bars. A small burr hole was drilled through the skull at 0.2 mm posterior and 2.2 mm lateral to the bregma, and a 26-gauge needle (Hamilton Company, Reno, NV, USA) was inserted into the hole to a depth of 3.5 mm from the skull surface. 1×10^5 luciferase-expressing U-87 MG cells suspended in ice-chilled PBS (1.5 μL) were intracranially implanted through the needle into the right striatum of the mice. The survival of animals was monitored daily and BLI was performed weekly.

In Vivo Brain Imaging in Normal Mice

Mice were anesthetized by intraperitoneal injection of 0.5% pentobarbital sodium (0.01 mL g^{-1}). 200 μL of TPN-cur (10 μg curcumin/2 mg F-127), TPN-CbV (20 μg CbV/2 mg F-127), and TPN-cur/CbV (10 μg curcumin/20 μg CbV/2 mg F-127) were injected intravenously and the PL signal from the whole body, including the brain, was monitored at different time points.

Colony Forming Assay

Rat C6 malignant glioma cells were treated overnight with free curcumin (5 μg), TPN-CbV (10 μg CBV/1 mg F-127), and TPN-cur/CbV (5 μg curcumin/10 μg CBV/1 mg F-127), after which the cells were seeded in 35 mm dishes at 500 cells/dish and allowed to form colonies for ≈7 d. At the end of the incubation period, colonies of 50 cells or more were stained with crystal violet and counted using a stereo microscope. Experiments were performed in duplicate, and statistical significance was determined in comparison with the untreated control.

Evaluation of Gene Expression

Real-time quantitative PCR (Q-PCR) was used to quantitate TNF-α, and NF-κB gene expression in C6 glioma cell cultures. Approximately 1×10^6 C6 glioma cells mL^{-1} were treated overnight with free curcumin, TPN-CbV, and TPN-cur/ CbV alone. After incubation, cytoplasmic RNA was extracted by an acid guanidinium-thiocyanate-phenol-chloroform method using Trizol reagent (Invitrogen- Life Technologies, Carlsbad, CA), and the amount of RNA was quantitated using a Nano-Drop ND-1000 spectrophotometer (Nano-Drop, Wilmington, DE). The extracted RNA was reverse transcribed to cDNA using a reverse transcriptase kit (Promega Inc, Madison, WI) by following the manufacturer's instruction. The relative abundance of each mRNA species was quantitated by normalizing the expression levels of each mRNA to the endogenous β-actin levels. Q-PCR was done using specific primers and the Brilliant SYBR green Q-PCR master mix (Stratagene Inc., La Jolla, CA). Q-PCR was performed in a reaction volume of 25 μL. Briefly, 12.5 μL of master mix, 2.5 μL of assay primers (10×), and 10 μL of template cDNA (100 ng) were added to each well. After a short centrifugation, the PCR plate was subjected to 35 cycles under the following conditions: (i) PCR activation at 95 °C for 5 min, (ii) denaturation at 95 °C for 5 s, and (iii) annealing/extension at 60 °C for 10 s. All samples and controls were run in triplicate on a Stratagene MX3000P real-time PCR system. Primer sequences used were as follows: TNF-α 5′-AGAGGGAGAGAAGCAACTACA-3′ (Sense) and 5′-GGGTCAGTATGTGAGAGGAAGA-3′ (AntiSense), Amplicon 103 bp.; NF-κB 5′-CTCTCCCACAGATGTGCATAAA-3′ (Sense) 5′-TTACAGGCCGCTCAATCTTC-3′ (AntiSense), Amplicon 83 bp; and housekeeping gene β-actin 5′-TTCTACAATGAGCTGCGTGTG-3′ (Sense) and 5′-GGGGTGTTGAAGGTCTCAAA-3′ (Antisense), Amplicon 114 bp.

To provide a precise quantification of the initial target in each PCR reaction, the amplification plot was examined and the data were calculated as described. Relative expression of mRNA species was calculated using the comparative threshold cycle number (C_T) method.[24] Briefly, for each sample, a difference in C_T values (ΔC_T) was calculated for each mRNA by taking the mean C_T of duplicate tubes and subtracting the mean C_T of the duplicate tubes for the reference RNA (β-actin) measured on an aliquot from the same RT reaction. The ΔC_T for the treated sample was then subtracted from the ΔC_T for the untreated control sample to generate a $\Delta\Delta C_T$. The mean of these $\Delta\Delta C_T$ measurements was then used to calculate the levels in the targeted cytoplasmic RNA relative to the reference gene and normalized to the control as follows: relative levels or transcript accumulation index = $2^{-\Delta\Delta C_T}$. This calculation assumes that all PCR reactions are working with 100% efficiency. All PCR efficiencies were found to be >95%; therefore, this assumption introduced minimal error into the calculations.

Cytotoxicity Assay

Cell viability was measured using the MTT colorimetric assay. Cells were seeded in 96-well plates and were cultured at 37 °C under 5% CO_2 for 24 h. Subsequently, serial dilutions (1, 0.5, 0.1 mg) of all three samples (F-127, TPN-cur, TPN-cur/CbV) were added to the culture medium, and cells were incubated for 24 h. 50 μL of a 0.5 mg mL^{-1} solution of MTT reagent dissolved in PBS was added to each well and the plates were incubated for an

additional 3 h at 37 °C. After 3 h incubation, the medium containing MTT was removed and 150 μL of DMSO was added to each well to dissolve the MTT formazan crystals formed. Finally, the plates were shaken for 10 min and MTT efficacy was measured by reading the 96-well plate on a microtiter plate reader (OptiMax, Molecular Devices) at an absorbance of 570 nm, with higher absorbance indicating higher cell survival. The results were plotted as percent survival compared with the corresponding control experiment results. Each data point represents the mean from a typical experiment with four replicate wells.

Immunofluorescent Staining

Approximately 5000 C6 glioma cells were grown on 35 mm glass-bottomed dishes and were treated overnight with free curcumin (5 μg), TPN-CbV (10 μg CBV/1 mg F-127), and TPN-cur/ CbV (5 μg curcumin/10 μg CBV/1 mg F-127). After incubation, cells were fixed with 3% paraformaldehyde for 10 min, blocked with 3% BSA, and incubated at 37 °C for 1 h with the primary anti-BCL-x rabbit polyclonal antibody (Cat # sc-7195, Santacruz Biotech, USA). The primary antibody was used in a dilution of 1:200, and an Alexa Fluor 488 conjugated donkey antirabbit secondary antibody (Cat # A-21206, Molecular Probes; Life Technologies, Grand Island, NY) was used in a dilution of 1:1000. DAPI (4′-6-diamidino-2-phenylindole, Cat # D1306, Molecular Probes; Life Technologies, Grand island, NY) was used to counterstain cell nuclei at a dilution of 1:400. Imaging was performed with the EVOS FL Cell Imaging System (Life Technologies, Grand Island, NY), and the expression levels of BCl-x were quantitated based on the intensity of the fluorescence signal analyzed by ImageJ software (National Institutes of Health, Bethesda, MA, USA).

In Vivo Brain Tumor Imaging in Mice Bearing Luciferase-Expressing U-87 MG Cells

Mice were anesthetized by intraperitoneal injection with a Zoletil and Rompun anesthetic cocktail and imaged 20 min after intraperitoneal injection of 150 mg kg^{-1} luciferin dissolved in PBS. 200 μL of TPN-CbV (20 μg CbV/2 mg F-127), was injected intravenously into the same mouse and the PL signal from the brain was monitored at different time points. In vivo imaging was performed via a Xenogen IVIS Lumina System (Caliper, USA) coupled with Living Image software for data acquisition. All animal experiments were carried out in accordance with the National Institutes of Health guide for the care and use of laboratory animals.

In Vivo Brain Tumor Imaging and Therapy

The first group of brain-tumor-wearing mice was treated with empty F-127 nanoparticles and the second group with 50 μg mL^{-1} of TPN-cur (0.5 mg/kg) each day. The tumor volume was measured every week by intraperitoneal injection of luciferin (150 mg kg^{-1} in PBS) and imaged 20 min after injection. Pseudocolor images, which represent photon intensity as blue (least intense) and red (most intense), were generated, and signal intensity was quantified within a region of interest over the right hemisphere that was defined by the Living Image software.

Supplementary Material

Refer to Web version on PubMed Central for supplementary material.

Acknowledgments

This work was supported by grants from the National Research Foundation of Korea (2014M3A9E5073316, 2014M3C1A3054141), the Korea Health Industry Development Institute (HI15C1540), the Development of Platform Technology for Innovative Medical Measurements Program from Korea Research Institute of Standards and Science (KRISS–2016-16011064), and the Intramural Research Program of KIST. The work at Buffalo was supported by grants from NIH (1R21EY026411-01) and from SUNY Brain Initiative (1127716-1-72697).

References

1. Abbott NJ, Rönnbäck L, Hansson E. Nat Rev Neurosci. 2006; 7:41. [PubMed: 16371949]
2. Obermeier B, Daneman R, Ransohoff RM. Nat Med. 2013; 19:1584. [PubMed: 24309662]
3. Nersesyan H, Slavin KV. Ther Clin Risk Manage. 2007; 3:381.
4. Miller DW, Batrakova EV, Waltner TO, Alakhov VY, Kabanov AV. Bioconjugate Chem. 1997; 8:649.
5. Batrakova EV, Li S, Vinogradov SV, Alakhov VY, Miller DW, Kabanov AV. J Pharmacol Exp Ther. 2001; 299:483. [PubMed: 11602658]
6. Kabanov AV, Batrakova EV, Miller DW. Adv Drug Deliv Rev. 2003; 55:151. [PubMed: 12535579]
7. Kelkar SS, Reineke TM. Bioconjugate Chem. 2011; 22:1879.
8. Jin M, Yu D-G, Geraldes CFGC, Williams GR, Annie Bligh SW. Mol Pharm. 2016; 13:2457. [PubMed: 27280491]
9. Chandana SR, Movva S, Arora M, Singh T. Am Fam Physician. 2008; 77:1423. [PubMed: 18533376]
10. Schneider SW, Ludwig T, Tatenhorst L, Braune S, Oberleithner H, Senner V, Paulus W. Acta Neuropathol. 2004; 107:272. [PubMed: 14730455]
11. Ewing JR, Brown SL, Lu M, Panda S, Ding G, Knight RA, Cao Y, Jiang Q, Nagaraja TN, Churchman JL, Fenstermacher JD. J Cereb Blood Flow Metab. 2006; 26:310. [PubMed: 16079791]
12. Wei KC, Chu PC, Wang HY, Huang CY, Chen PY, Tsai HC, Lu YJ, Lee PY, Tseng IC, Feng LY, Hsu PW, Yen TC, Liu HL. PLoS One. 2013; 8:e58995. [PubMed: 23527068]
13. Kim W, Kim HY, Woo J, Rhim HJ, Kang BR, Lee YD, Kim S, Kim JY, Choi EJ, Kim KS, Kim DJ, Kim Y. Bull Korean Chem Soc. 2015; 36:1528.
14. Rahmani AH, Al Zohairy MA, Aly SM, Khan MA. Biomed Res Int. 2014; 2014:1.
15. Sa G, Das T. Cell Div. 2008; 3:1. [PubMed: 18179693]
16. Anand P, Kunnumakkara AB, Newman RA, Aggarwal BB. Mol Pharm. 2007; 4:807. [PubMed: 17999464]
17. Singh A, Lim CK, Lee YD, Maeng J, Lee S, Koh J, Kim S. ACS Appl Mater Interfaces. 2013; 5:8881. [PubMed: 23731221]
18. Singh A, Seo YH, Lim CK, Koh J, Jang WD, Kwon IC, Kim S. ACS Nano. 2015; 9:9906. [PubMed: 26316392]
19. Albanese A, Tang PS, Chan WCW. Annu Rev Biomed Eng. 2012; 14:1. [PubMed: 22524388]
20. Mahajan SD, Aalinkeel R, Sykes DE, Reynolds JL, Bindukumar B, Adal A, Qi M, Toh J, Xu G, Prasad PN, Schwartz SA. Brain Res. 2008; 1203:133. [PubMed: 18329007]
21. Patra D, Barakat C. Spectrochim Acta Mol Biomol Spectrosc. 2011; 79:1034.
22. Franken NA, Rodermond HM, Stap J, Haveman J, Bree CV. Nat Protoc. 2006; 1:2315. [PubMed: 17406473]
23. Tiffen JC, Bailey CG, Ng C, Rasko JE, Holst J. Mol Cancer. 2010; 9:1. [PubMed: 20051109]
24. Bustin SA. J Mol Endocrinol. 2002; 29:23. [PubMed: 12200227]

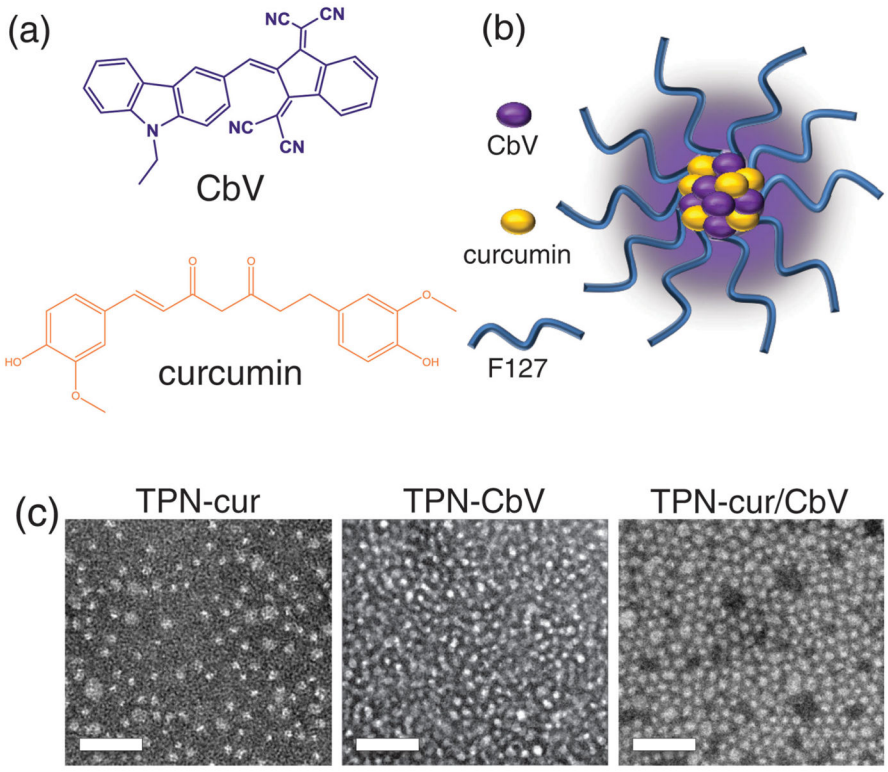

Figure 1.

a) Chemical structures of photonic molecules employed in this study, and b) schematic representation of TPN. c) TEM images of curcumin and/or CbV-loaded TPNs. Scale bars: 100 nm.

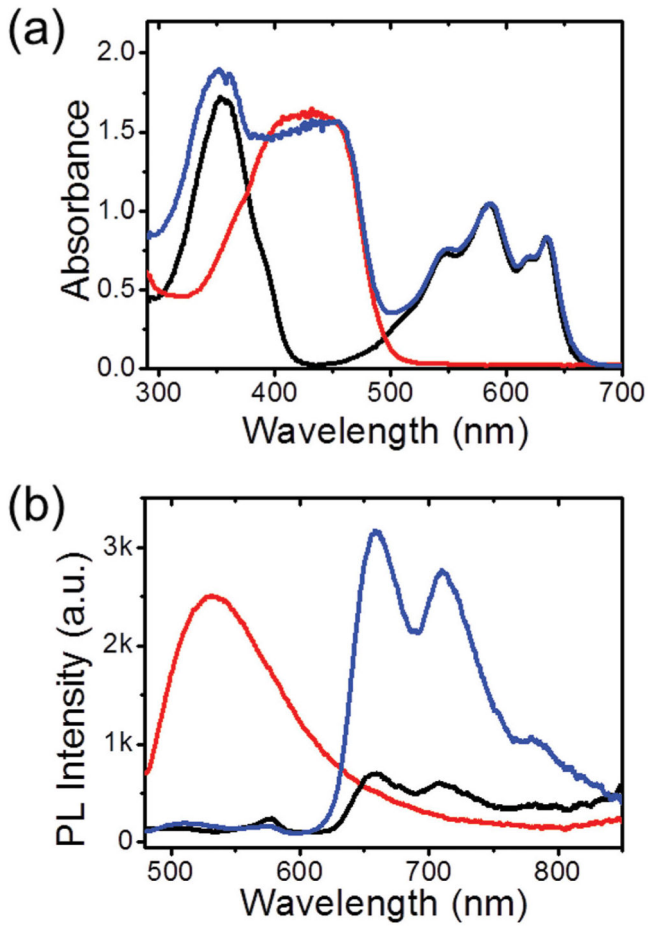

Figure 2.

a) Absorption and b) photoluminescence (PL, excited at 450 nm) spectra of TPN-cur (red line), TPN-CbV (black line), and TPN-cur/CbV (blue line) in water.

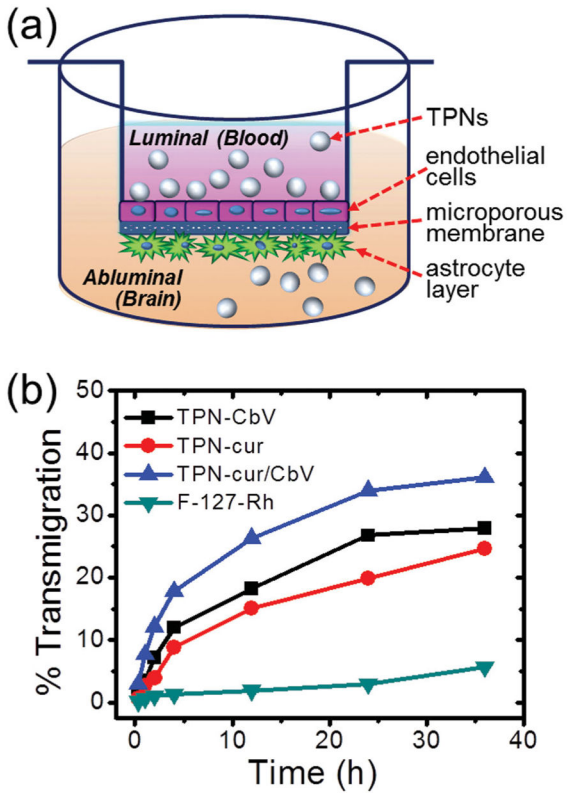

Figure 3.

a) Schematic diagram of in vitro BBB model. b) Percentage transmigration of TPNs and disseminated F-127 (F-127-Rh) across the in vitro BBB.

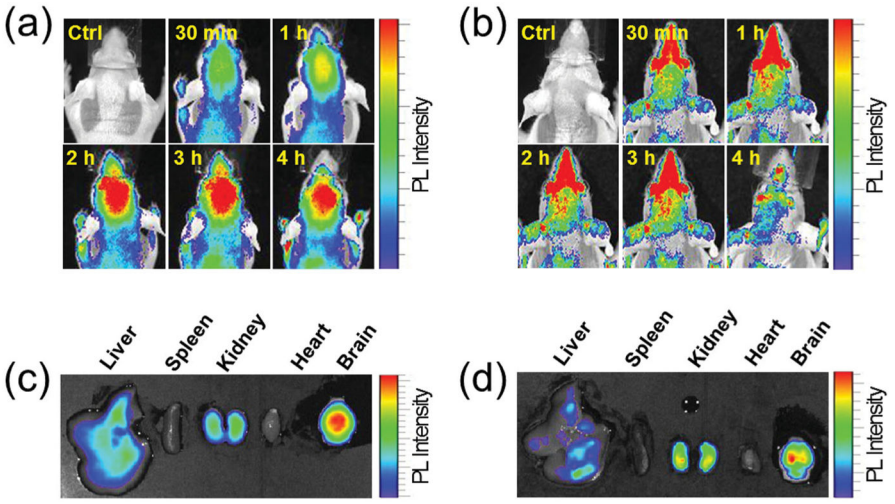

Figure 4.

a,b) In vivo imaging of temporal signals from TPNs intravenously injected to normal mice, and c,d) ex vivo images of major organs resected at 4 h postinjection: TPN-CbV (a,c) and TPN-cur (b,d). Imaging time points after sample injection are indicated in the in vivo images.

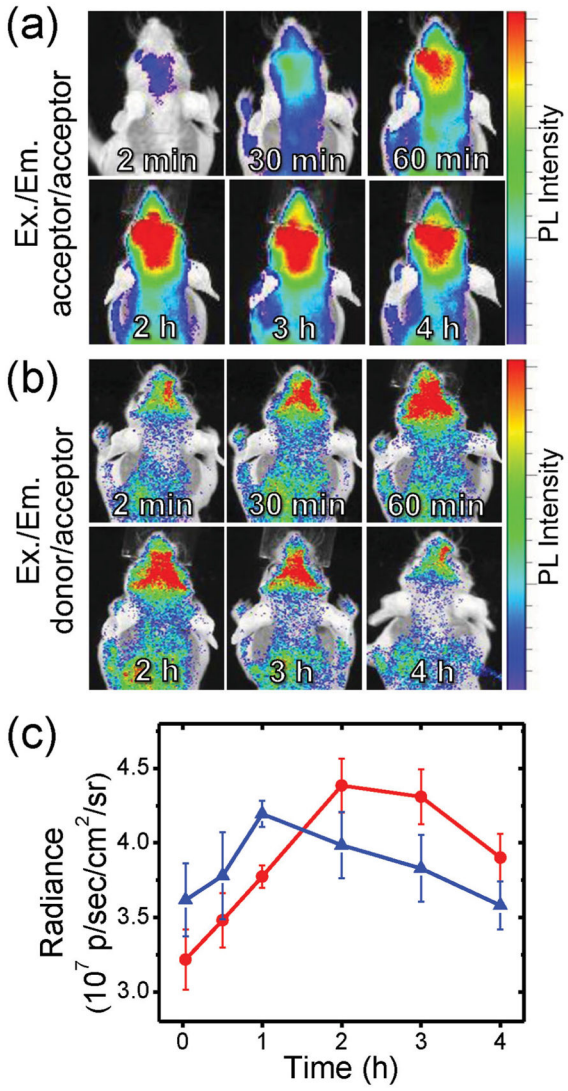

Figure 5.

a,b) In vivo imaging of temporal signals from TPN-cur/CbV intravenously injected in normal mice ($n = 3$). Excitation/emission wavelengths are a) 640 nm/700 nm (direct excitation) and b) 500 nm/700 nm (energy-transferred indirect excitation). Imaging time points after sample injection are indicated. c) Signal intensity profiles of direct excitation (red line) and energy-transferred indirect excitation (blue line).

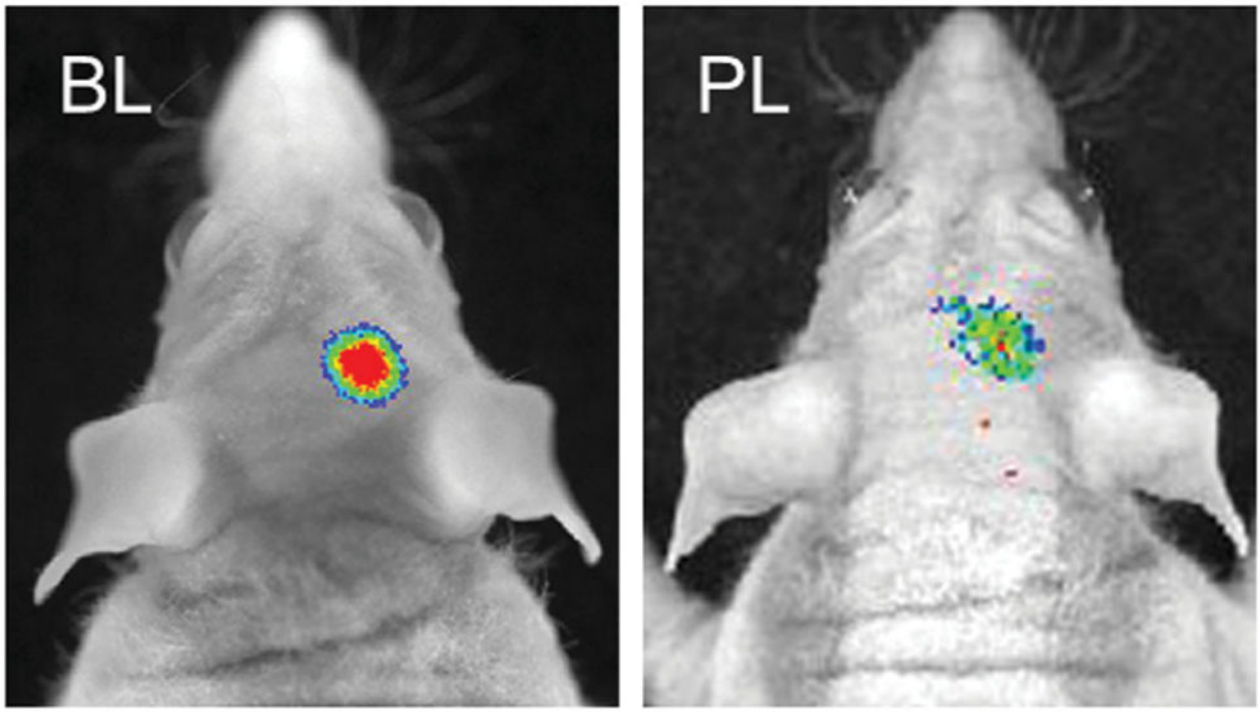

Figure 6.

In vivo imaging of bioluminescent GBM xenograft in an orthotopic mouse model. Tumor bioluminescence (BL) and TPN photoluminescence (PL) were imaged at 30 min after intravenous injection of luciferin and TPN-CbV, respectively.

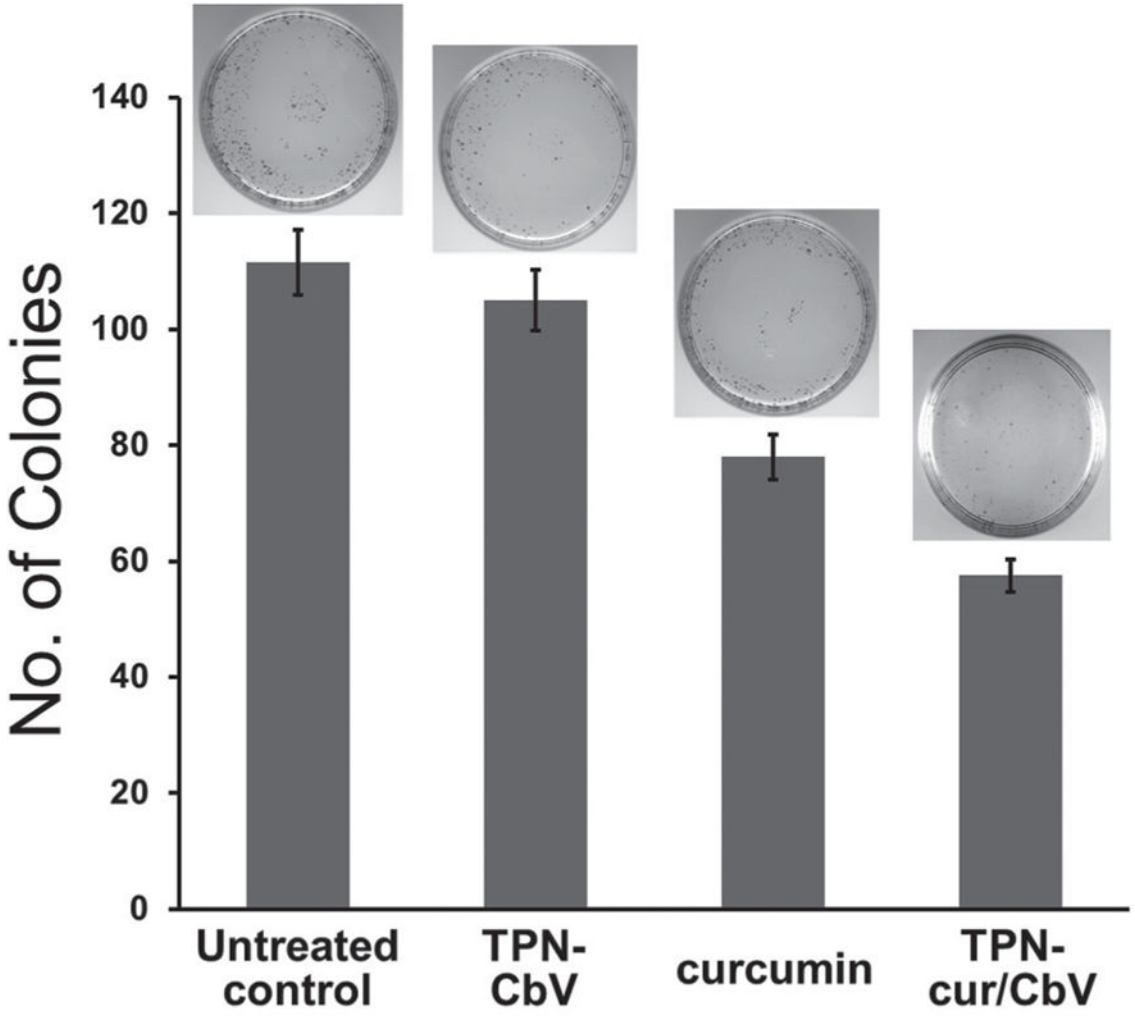

Figure 7.

Suppressive effects of TPN-CbV, curcumin, and TPN-cur/CbV on colony formation of rat C6 malignant glioma cells ($n = 3$). The insets are representative images of colony-forming assay.

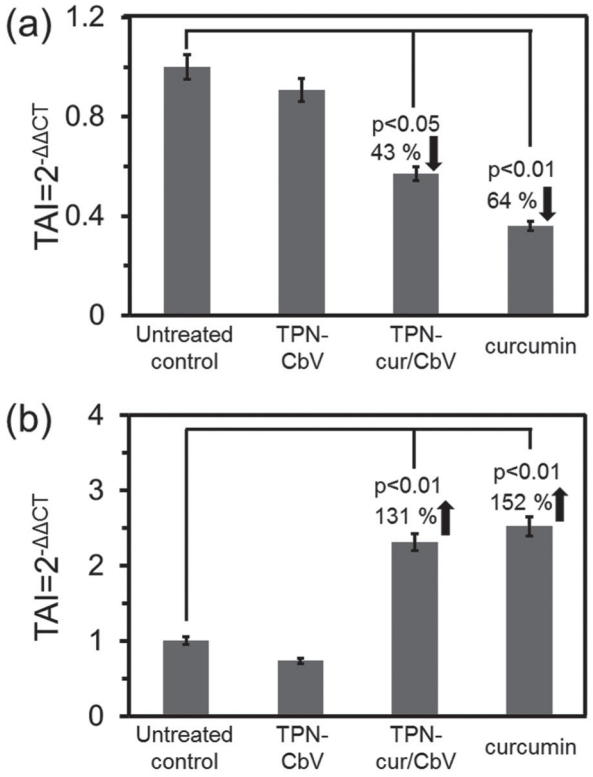

Figure 8.

Effects of TPN-CbV, curcumin, and TPN-cur/CbV on gene expression levels of a) TNF-α and b) NF-κB in rat C6 malignant glioma cells treated with each sample for 24 h. RNA was extracted, reverse transcribed, and subjected to real-time Q-PCR. Results are expressed as the mean ± SD from separate experiments ($n = 3$). A p value of <0.05 is considered a statistically significant difference.

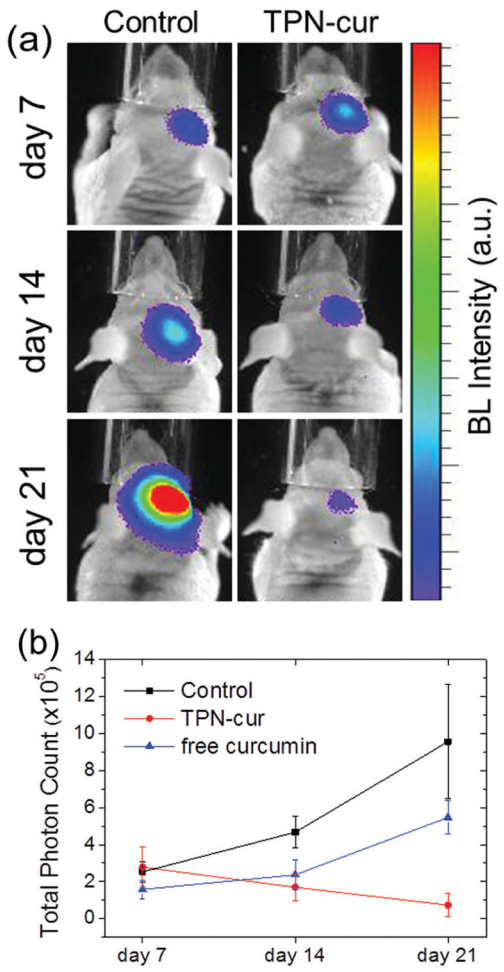

Figure 9.

a) In vivo images and b) temporal trace of bioluminescence from GBM xenograft in an orthotopic mouse model intravenously injected with TPN-cur or F-127 (Control), and intraperitoneally with free curcumin in DMSO solution (b). Luciferin-induced tumor bioluminescence, reflecting the level of GBM proliferation, was imaged at the indicated time points with daily sample-treated mice ($n = 3$).